

---

# Travelling waves in a straight square duct

M. Uhlmann<sup>1</sup>, G. Kawahara<sup>2</sup> and A. Pinelli<sup>3</sup>

<sup>1</sup>Institut für Hydromechanik, Universität Karlsruhe, 76131 Karlsruhe, Germany

<sup>2</sup>Department of Mechanical Science, Osaka University, 560-8531 Osaka, Japan

<sup>3</sup>Modeling and Numerical Simulation Unit, CIEMAT, 28040 Madrid, Spain

markus.uhlmann@ifh.uka.de

## 1 Introduction

Isothermal, incompressible flow in a straight duct with square cross-section is known to be linearly stable [1]. Direct numerical simulation, on the other hand, has revealed that turbulence in this geometry is self-sustained above a Reynolds number value of approximately 1100, based on the bulk velocity and the duct half-width [2].

Numerous non-linear equilibrium solutions have already been identified in plane Couette, plane Poiseuille and pipe flows [3, 4, 5], and their role in the transition process as well as their relevance to the statistics of turbulent flow have been investigated [6, 7, 8]. No non-linear travelling-wave solutions for the flow through a square duct have been published to date.

In the specific case of square duct flow, it can be anticipated that travelling wave solutions will help to shed further light on the origin of mean secondary flow, whose appearance has been linked to the near-wall coherent structures [2]. Here we will present results obtained by applying an iterative solution strategy to the steady Navier-Stokes equations in a moving frame of reference. In the absence of a “natural” primary bifurcation point, we resort to the method proposed by Waleffe [9], where streamwise vortices are artificially added to the base flow and forced against viscous decay, leading to streaks, which are in turn linearly unstable, feeding back into the original vortices. The non-linear solution is then continued back to the original problem, i.e. the unforced flow.

## 2 Numerical method

Our method is an extension of the classical spectral approach often used e.g. in plane channel flow [4]. Here we employ a primitive variable formulation. The dependent variables  $\varphi = \{u, v, w, p\}$  are expanded as follows:

$$\varphi(\mathbf{x}, t) = \sum_{n=-N_x}^{N_x} \sum_{m=0}^{N_y-k^{(\varphi)}} \sum_{l=0}^{N_z-k^{(\varphi)}} \varphi_{nml} \phi_m^{(\varphi)}(y) \phi_l^{(\varphi)}(z) \exp(in\alpha(x - ct)), \quad (1)$$

where  $\alpha$  is the streamwise wavenumber and  $c$  the (real-valued) phase speed and  $i = \sqrt{-1}$ . The functions  $\phi^{(\varphi)}$  are modified Chebyshev polynomials which incorporate odd/even parities and—in the case of  $\varphi$  being a velocity component—the wall boundary conditions. The pressure field has two polynomial degrees less than the velocity field, i.e.  $k^{(p)} = 2$  and  $k^{(u_i)} = 0$ . A Galerkin method is employed in the streamwise (Fourier) direction, and the collocation method is applied in the cross-stream (Chebyshev) directions. In our case, the collocation points for pressure are chosen as the *Gauss* points, i.e. pressure is staggered w.r.t. the usual *Gauss-Lobatto* grid used for velocity, thereby avoiding spurious pressure modes. The solution of the resulting non-linear algebraic system is performed via Newton-Raphson iteration; continuation is implemented by means of a standard arc-length procedure. The methodology has been validated by comparison with available data for plane channel flow [4]; our code also reproduces the linear results of [10] perfectly.

### 3 Results

Similar to what has been proposed in [9, 11] we construct the initial conditions for our non-linear procedure as a superposition of various ingredients: (i) the laminar base flow, (ii) streamwise rolls (taken as one of the least decaying eigenmodes of the Stokes operator on the square), (iii) the streaks induced by the rolls, and (iv) neutrally stable linear perturbations (with specific parities I to IV, according to the nomenclature of [1]) of the roll/streak flow. Contrary to [12] we have focused upon initial conditions constructed from roll/streak-instabilities with type-II and type-III parities. After continuing various initial fields towards a state with zero forcing we have obtained different families of travelling waves. In the following we will present results corresponding to the fourth Stokes mode and roll/streak-instabilities of type-II.

Figure 1(a) shows the perturbation energy of this solution family at various values for the streamwise wavenumber  $\alpha$ . Figure 1(b) shows that these three curves are cutting the solution region near the two extremes in  $\alpha$  (1.58 and 0.6) and around the center (1.0), with the lower wavenumbers leading to considerably higher perturbation energies. The smallest Reynolds numbers, however, are obtained close to  $\alpha = 1$ , for which this family yields  $Re_{b,min} \approx 600$ . Concerning the wall friction, it can be seen from the graph in figure 1(c) that values around and above the extrapolation from the turbulent regime are obtained for the travelling-waves with smaller streamwise wavenumber, with the lower branch yielding a flow near the laminar limit; for large wavenumbers, both upper and lower solution branch are only little removed from the laminar friction value. Figure 1(d) shows the energy of the secondary motion induced

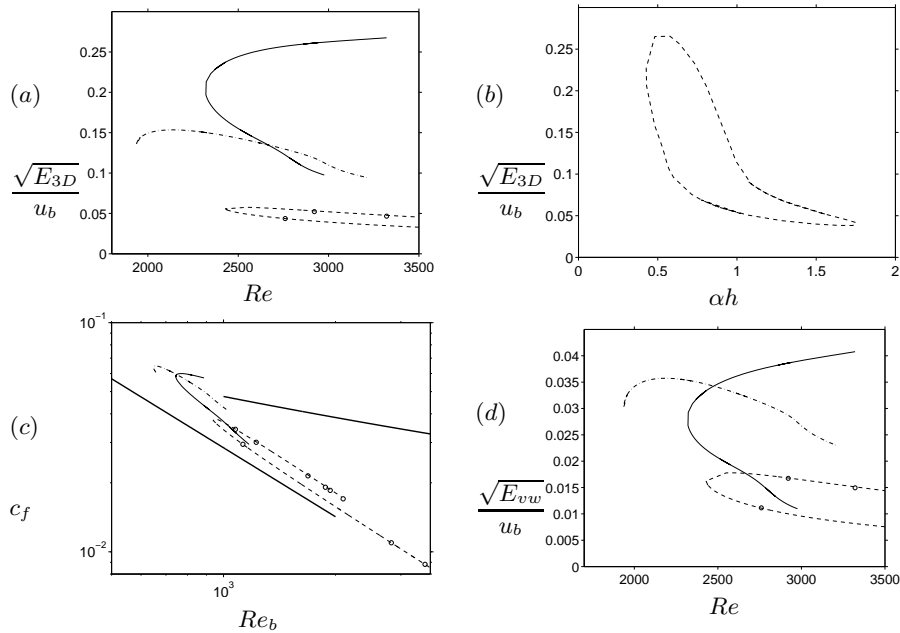


**Fig. 1.** Results for truncation levels  $N_x = 2$ ,  $N_y = N_z = 30$  (lines) and  $N_x = 4$ ,  $N_y = N_z = 32$  (symbols). In (a), (c), (d) the different lines correspond to wavenumber values: ----,  $\alpha = 1.58$ ; - · -,  $\alpha = 1.0$ ; —,  $\alpha = 0.6$ .  $E_{3D}$  is the total perturbation energy of the velocity field, excluding the streamwise constant mode;  $E_{vw}$  corresponds to the energy of the streamwise-averaged secondary flow. Whereas the other plots show continuation lines varying the value of the Reynolds number, the graph (b) shows a solution curve when varying  $\alpha$  with fixed  $Re = 3321$  (based on maximum base flow velocity). In (c) the thick straight lines indicate the friction factor for laminar and fully turbulent flow. Note that  $Re$  is the Reynolds number based upon the maximum laminar base flow velocity and duct half width.

by the travelling wave. As a comparison, in fully-turbulent flow at marginal Reynolds numbers ( $Re_b \approx 1100$ ) we have measured an intensity of  $\sqrt{E_{vw}}/u_b \approx 0.09$  [2], roughly twice as much as the largest value in figure 1(d). The shape of the streamwise averaged secondary flow is shown in figure 2(a), exhibiting eight streamwise vortices—similar to time-averaged turbulent flow. Figure 2(b) shows isosurfaces of the total streamwise velocity and of streamwise vorticity. The structure above an individual wall is very much alike the one obtained in a periodic cell of plane Poiseuille flow [9], with a single slightly undulating streak flanked by a pair of staggered streamwise vortices.

It can be concluded that the present family of travelling waves appears to be highly relevant to turbulent duct flow at low-Reynolds numbers. In fact, our solutions represent the first non-linear equilibrium state which exhibits eight-vortex secondary flow, and can therefore be expected to contribute to further

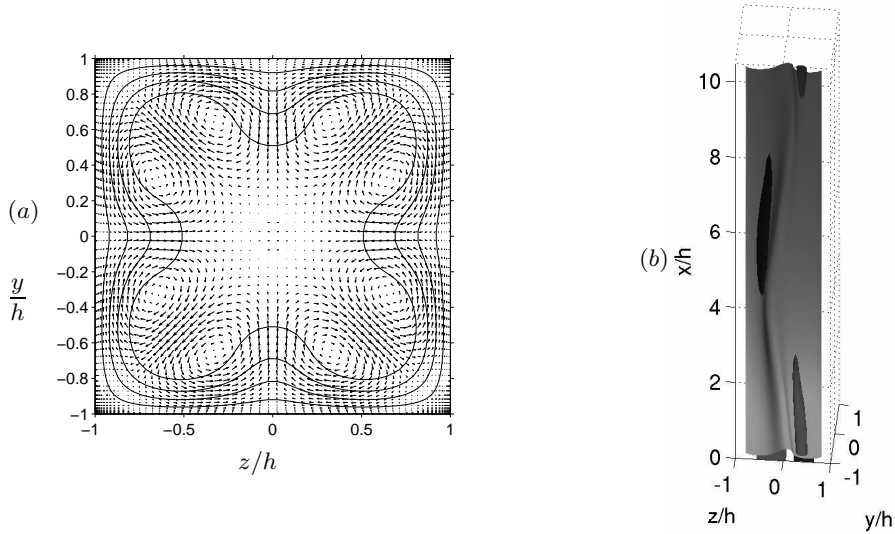


**Fig. 2.** Shape of a travelling wave on the upper branch at  $Re_b = 760$  and  $\alpha = 0.6$ , having a phase speed of  $c/u_b = 1.44$ . (a) Streamwise averaged secondary flow vectors and primary flow contours; (b) isosurfaces of  $u = 0.45 \max(u)$  (light grey sheet) and  $\omega_x = \pm 0.3 \max(\omega_x)$  (dark grey tubes) shown above one wall, with the other three sectors (delimited by the cross-sectional diagonals) cut away for clarity.

the understanding of the generation mechanism of secondary flow. In order to establish a direct link with turbulence, however, an in-depth investigation of its dynamical properties needs to be carried out.

## References

1. T. Tatsumi, T. Yoshimura: *J. Fluid Mech.* **212**, 437–449 (1990)
2. M. Uhlmann, A. Pinelli, G. Kawahara, A. Sekimoto: *J. Fluid Mech.* **588**, 153–162 (2007)
3. M. Nagata: *J. Fluid Mech.* **217**, 519–527 (1990)
4. U. Ehrenstein, W. Koch: *J. Fluid Mech.* **228**, 111–148 (1991)
5. H. Faisst, B. Eckhardt: *Phys. Rev. Lett.* **91**, (2003) art. 224502.
6. J. Jiménez, G. Kawahara, M. Siemens, M. Nagata, M. Shiba: *Phys. Fluids* **17**, 015105 (2005)
7. B. Eckhardt, T. Schneider, B. Hof, J. Westerweel: *Annu. Rev. Fluid Mech.* **39**, 447–468 (2007)
8. J. Gibson, J. Halcrow, P. Cvitanović: *J. Fluid Mech.* **611**, 107–130 (2008)
9. F. Waleffe: *Phys. Fluids* **15**, 1517–1534 (2003)
10. M. Uhlmann, M. Nagata: *J. Fluid Mech.* **551**, 387–404 (2006)
11. H. Wedin, R. Kerswell: *J. Fluid Mech.* **508**, 333–371 (2004)
12. H. Wedin, D. Biau, A. Bottaro, M. Nagata: *Phys. Fluids* **20**, 094105 (2008)